Clinical Neurophysiology 120 (2009) 1787–1796

Contents lists available at ScienceDirect

Clinical Neurophysiology

journal homepage: www.elsevier.com/locate/clinph

Neonatal seizure localization using PARAFAC decomposition

W. Deburchgraeve [a,*], P.J. Cherian [b], M. De Vos [a], R.M. Swarte [c], J.H. Blok [b], G.H. Visser [b], P. Govaert [c], S. Van Huffel [a]

[a] Department of Electrical Engineering (ESAT), Katholieke Universiteit Leuven, Kasteelpark Arenberg 10, 3001 Leuven-Heverlee, Belgium
[b] Department of Clinical Neurophysiology, Erasmus MC, University Medical Center Rotterdam, 's-Gravendijkwal 230, 3015 CE, Rotterdam, The Netherlands
[c] Department of Neonatology, Sophia Children's Hospital, Erasmus MC, University Medical Center Rotterdam, Dr. Molewaterplein 60, 3015 GJ, Rotterdam, The Netherlands

ARTICLE INFO

Article history:
Accepted 29 July 2009
Available online 6 September 2009

Keywords:
Neonate
Electroencephalography (EEG)
Seizure localization
PARAFAC

ABSTRACT

Objective: The description and evaluation of two EEG-based algorithms for automatic and objective determination of the seizure location in the neonatal brain as it is reflected on the scalp.
Methods: Each algorithm extracts the electrical potential distribution of the seizure over the scalp using the higher-order canonical decomposition or Parallel Factor Analysis (PARAFAC), also referred to as the CP model. This model decomposes a tensor in a sum of rank-1 components. The two algorithms differ in the way the tensor is constructed and in the type of activity they are able to extract. While the first method extracts oscillatory seizure activity, the second extracts spike train activity.
Results: We compared the seizure localization results of 21 seizures from 6 neonates with post-asphyxial hypoxic ischemic encephalopathy, with that based on the visual analysis of the EEG by a clinical neurophysiologist. There was a good agreement between the two methods in the localization of seizure onset in all.
Conclusion: The techniques presented in this paper are robust, objective methods to determine neonatal seizure localization. They can be a useful tool for neonatal EEG analysis and for continuous brain function monitoring.
Significance: The proposed algorithms significantly improve neonatal seizure localization and monitoring.
© 2009 International Federation of Clinical Neurophysiology. Published by Elsevier Ireland Ltd. All rights reserved.

1. Introduction

Neonatal seizures are the most frequent major manifestation of neonatal neurological disorders (Lanska and Lanska, 1996; Volpe, 2008). The majority of the seizures occurring in neonates admitted to the neonatal intensive care unit (NICU) are subclinical, being detected only by EEG monitoring (Hellstrom-Westas et al., 1985; Scher et al., 1989; Murray et al., 2008). Interpretation of the neonatal EEG requires specific expertise, which is normally not present around the clock in the NICU. Long-term EEG monitoring accumulates large amounts of data and its interpretation is labor-intensive. Therefore, there is a need for automated monitoring techniques that allow reliable extraction of the relevant information in the EEG. This allows faster decision making without the need for constant on-site expert supervision.

Recently, we developed an automated EEG-based neonatal seizure detection method (Deburchgraeve et al., 2008). For this detection method, we divided the neonatal seizures into two morphological types with respect to their EEG characteristics, and for each, a different detection strategy was developed. The first is the oscillatory type, which consists of a continuous oscillating pattern (Fig. 1(B)). The second is the spike train type, i.e., a train of isolated repetitive spikes in the EEG (Fig. 1(A)). After detection, it is important to determine which brain region is involved. An assessment of the location and number of seizure foci in neonatal EEG may help in identifying the injured areas of the brain, as well as in prognostication (Pisani et al., 2008, 2009). It could also be of help in a future scenario of guiding targeted therapies for different types of brain injuries in the NICU. Seizure location can be determined by visual interpretation of the raw EEG, but this approach is time-consuming and suffers from considerable interrater variability. Simple EEG trends, such as the single-channel amplitude integrated EEG (aEEG) that is used in many NICUs, are sub-optimal for the detection of seizures (Rennie et al., 2004). More importantly, they do not provide spatial information regarding the detected seizures.

* Corresponding author. Address: Department of Electrical Engineering (ESAT), Katholieke Universiteit Leuven, Kasteelpark Arenberg 10, P.O. Box 02446, 3001 Leuven-Heverlee, Belgium. Tel.: +32 (0) 498 08 56 76.
E-mail address: wouter.deburchgraeve@esat.kuleuven.be (W. Deburchgraeve).

1388-2457/$36.00 © 2009 International Federation of Clinical Neurophysiology. Published by Elsevier Ireland Ltd. All rights reserved.
doi:10.1016/j.clinph.2009.07.044

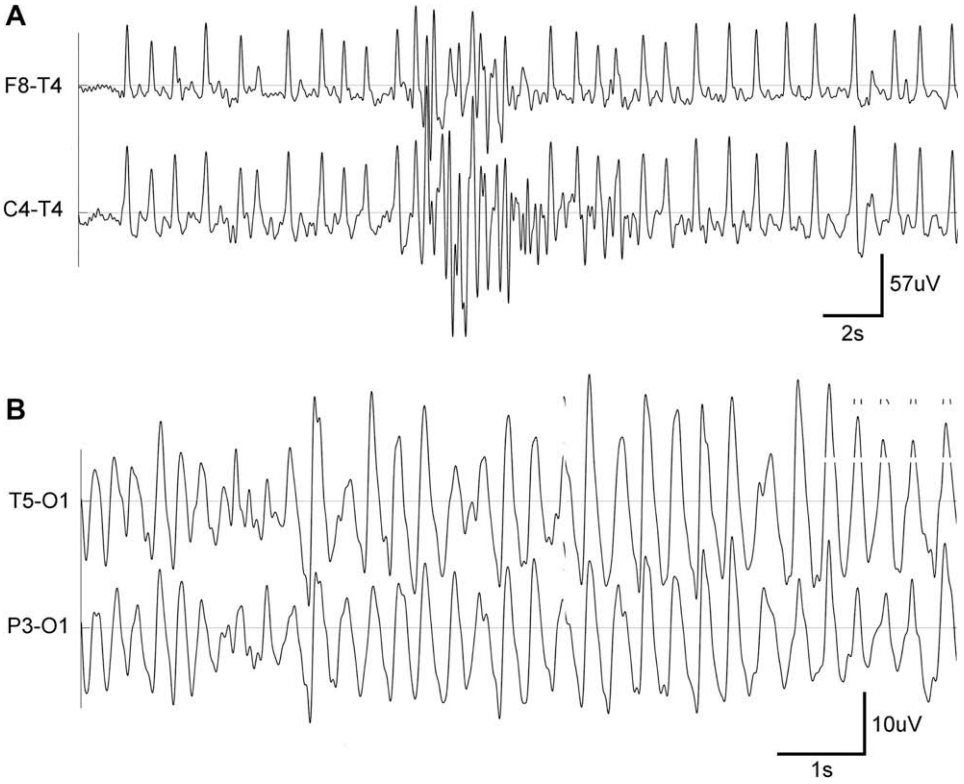


Fig. 1. (A) Example of a spike train type seizure, (B) example of an oscillatory type seizure.

This paper is the first to provide a robust and objective localization method for neonatal seizures. The method is based on Canonical Decomposition (CANDECOMP), also known as Parallel Factor Analysis (PARAFAC), often referred to as the CP (CANDECOMP/PARAFAC) decomposition. Most decomposition methods applied to EEG, such as, PCA (Principal Component Analysis) (Kovacevic and McIntosh, 2007), ICA (Independent Component Analysis) (Patel et al., 2008), and CCA (Canonical Correlation Analysis) (De Clercq et al., 2006), can only be applied to 2-dimensional data arrays. With CP decomposition, it is possible to decompose higher dimensional data arrays or tensors (Smilde et al., 2004).

The CP decomposition for EEG analysis was introduced fairly recently (Miwakeichi et al., 2004). Subsequent work (De Vos et al., 2007a; Acar et al., 2007) has shown that the CP decomposition can provide a reliable estimate of the epileptic seizure onset zone in the EEG of adults, even in the presence of disturbing artefacts. In the present paper, we propose two methods based on CP decomposition to localize the neonatal seizures. The first one is based on previous work in the literature and used to localize the oscillatory seizures as detected by the seizure detector. For convenience, in the remainder of this paper, we will refer to this method as O-CP (Oscillatory CP). The second is a new method specialized in localizing the spike train type of seizures. This method employs the output of the previously developed spike train detector (Deburchgraeve et al., 2008) and will be referred to as SP-CP (Spike Train CP).

2. Materials and methods

2.1. Data set

All EEG data were recorded at the Sophia Children's Hospital (part of the University Medical Center Rotterdam, the Netherlands). The data consisted of a representative set of 21 seizures extracted from 6 different patients with perinatal asphyxia and HIE. These six were part of the 21 patients described in our previous study (Deburchgraeve et al., 2008). EEG registrations were made with silver–silver chloride electrodes applied on the scalp according to the 10–20 International System (17 electrodes: Fp1,2, F3,4, C3,4, Cz, P3,4, F7,8, T3,4, T5,6, O1,2) using conductive paste and fixed with collodion. Each measurement started within 24 h of birth. Sampling frequency was 256 Hz. The seizures were scored and localized by an experienced clinical neurophysiologist. Before analysis, the data was filtered between 0.3 and 30 Hz. We used the previously developed seizure detector to automatically select the EEG segments to be used for localization.

2.2. Methods

We start by introducing the CP decomposition (2.2.1). We then describe the O-CP (2.2.2) and the SP-CP methods (2.2.3) in detail. Next, we describe the existing spike triggered averaging method (Bast et al., 2006; Braga et al., 2002) (2.2.4) and compare the performance of this method to the new SP-CP method. We illustrate the application of both methods to localize neonatal seizures (3.1 and 3.2). By means of simulations, we compare the robustness to noise of the SP-CP method with that of spike triggered averaging (3.3).

2.2.1. CP decomposition

The trilinear CP model for a three-way array $X^{(I\times J\times K)}$ is given by:

$$x_{ijk} = \sum_{r=1}^{R} a_{ir} b_{jr} c_{kr} + e_{ijk} \quad (1)$$

where R is the number of components used in the CP model, and e_{ijk} are the residuals containing the unexplained variation. A pictorial representation of the CP decomposition with R atoms is given in Fig. 2.

The CP model is a trilinear model: fixing the parameters in two modes, x_{ijk} is expressed as a linear function of the remaining parameters.

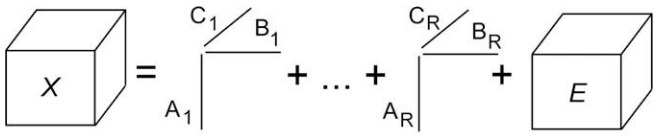


Fig. 2. Pictorial representation of the CP decomposition of a 3-dimensional tensor with R atoms.

The CP decomposition was originally computed by means of an Alternating Least Squares (ALS) algorithm (Smilde et al., 2004). Although several alternatives to ALS have been described, we used ALS as it has not yet been proven that the new methods provide a better accuracy (Tomasi and Bro, 2006). This means that the least-squares cost function

$$f(A,B,C) = \|X - \sum_{r=1}^{R} A_r \circ B_r \circ C_r\|^2 \quad (2)$$

is minimized by means of alternating updates of one of its matrix arguments, keeping the other two matrices fixed. Because the CP decomposition is a multi-linear decomposition, each update just amounts to solving a classical linear least-squares problem (Smilde et al., 2004).

CP decomposition models the variance in the tensor as well as possible with a predefined number of trilinear structures. As we would like each trilinear structure to represent a distinct brain source, it is important that the sources we want to extract from the tensor are adequately modeled with such a trilinear structure. Otherwise, the CP decomposition will not be able to separate them. Basically, the trilinear structure allows us to "catch" three aspects of seizure activity that differentiate it from background activity. In addition to the EEG channels involved (localization of the seizure) and the time (time course of the seizure), we use the third dimension to characterize the oscillatory (for O-CP) or repetitive (for SP-CP) nature of the seizure. The two methods presented in this paper differ in the construction of the third dimension of the tensor, as they need to extract a different type of activity (oscillations as opposed to spikes).

2.2.2. O-CP decomposition method

This method is designed to localize the oscillatory type of neonatal seizures (Fig. 1(B)). The seizure needs to be completely separated from all other concurrent EEG activity which might also be oscillatory. We will show that the way we construct the tensor makes the trilinear structure of the CP decomposition suitable for localizing oscillatory sources as reflected in the scalp EEG.

The third dimension of the tensor is constructed using the continuous wavelet transform of the ongoing EEG recording (Miwakeichi et al., 2004). Consequently, the tensor consists of the dimensions channels, time, and frequency. We computed the decomposition on the 'pure' wavelet-transformed EEG in contrast to previous studies, where the CP decomposition was calculated using the power (square) of the wavelet-transformed EEG.

The wavelet transform is chosen for its optimal time-frequency resolution. Wavelets resolve high frequency components within small time windows and low frequencies in larger time windows. The continuous wavelet C at scale a and time t of a signal $x(t)$ is defined by

$$C(a,\text{time}) = \int_{-\infty}^{\infty} x(t)\phi(a,\text{time},t)dt \quad (3)$$

with ϕ the chosen wavelet. In this study, we used a biorthogonal wavelet with decomposition order 3. The exact choice of the wavelet does not really affect the result. From the scale a of the wavelet, the frequency f of the signal can be estimated as:

$$f = \frac{f_c}{a\Delta t} \quad (4)$$

with f_c the center frequency of the wavelet and Δt the sampling period.

We took those frequency components that had a center frequency f_c ranging from 1 Hz up to 30 Hz with a step of 1 Hz. The corresponding wavelet scale a for each of these frequency components was calculated using Eq. (4). This means that the tensor was constructed using wavelet coefficients with a linear increase in center frequency instead of using coefficients with a linear increase in scale a. If we had chosen the frequency components to be linear in a, the tensor would have contained mainly low frequency components, resulting in an unwanted tendency to favor these components in the CP decomposition.

After construction of the tensor as described above, it was decomposed using an R-component CP decomposition. The suitable number of components was determined by checking the Core Consistency Diagnostic (Smilde et al., 2004). We found the optimal number of components to be two. Thus, each decomposition led to two trilinear components, i.e., two extracted time vectors (B_1 and B_2, see Fig. 3(A)), two spatial distribution vectors (A_1 and A_2) containing the spatial distribution of the extracted time series, and two frequency distribution vectors (C_1 and C_2) representing the frequency content of the extracted time series. For localization purposes, the A-components or the spatial vectors containing the distribution weights of the extracted activity over the EEG channels were the most relevant. We visualized this vector using topographic plots that showed the distribution on the scalp.

2.2.3. SP-CP decomposition

This algorithm is designed to localize neonatal spike train type seizures. Instead of using the complete EEG segment to construct the tensor as in the O-CP method, here we make use of the output of the spike train seizure detector (Deburchgraeve et al., 2008). The output of this detector consists of a series of segmented spikes. The goal is to use all spikes available to robustly localize the origin of the detected seizure. Using multiple spikes is better than single spike localization as the latter is strongly dependent on the signal-to-noise ratio (SNR), that is, the ratio of spike to background EEG amplitudes (Bast et al., 2006). The method we developed, based on CP tensor decomposition, analyzes all spikes simultaneously. The first two dimensions of the tensor again are EEG channels and time. Instead of using the frequency information, the third dimension is now built up by aligning all EEG segments (taking all channels) of the detected spikes one after the other in different slices of the tensor (see Fig. 3(B)). The third dimension of the tensor thus consists of an aligned set of EEG slices. Before the detected spikes can be added to the tensor, they need to be standardized and properly aligned to each other. This is done by the following procedure:Divide the spike segment by the maximum value of the EEG segment and subtract the mean over all channels.Shift the detected segments to align the maximum values of all the spikes to each other.Multiply each detected spike segment with a Hamming window

Add zeros before and after each detected spike segment until the length of each spike segment is equal to the length of the longest segment to be added to the tensor.Arrange all EEG segments after each other to construct the tensor.

The zeros added in step 4 are necessary because the lengths of the EEG segments of the detected spikes are not identical. After the zeros are added, each segment has equal length and a proper tensor can be constructed. This addition of zeros has no influence on the outcome of the CP decomposition and does not distort the localization. The Hamming window in step 3 is necessary because the addition of the zeros would otherwise lead to a discontinuity at

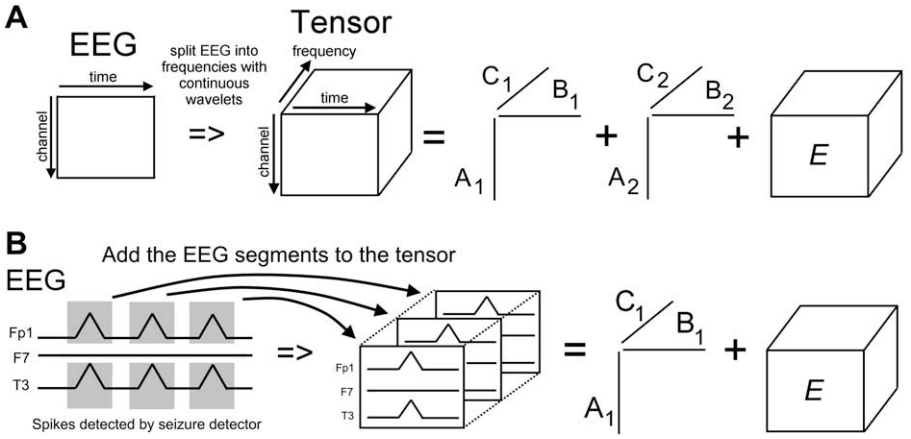


Fig. 3. (A) Localization of oscillatory type seizures: The third dimension of the tensor was constructed by decomposing the 2D EEG (channel and time) into a set of frequency components using continuous wavelets. After the tensor is built up, a two-component CP decomposition is calculated. (B) Localization of spike train type seizures: The spikes as detected and segmented by the seizure detector are added to the tensor. After the tensor is built up, a one-component CP decomposition is calculated.

the boundaries of the signal. The Hamming window forces the boundaries of the signal to zero, eliminating the gap.

After construction of the complete tensor, it was decomposed with a one-component CP decomposition. We only needed one-component as the tensor only contains seizure data. The one-component trilinear structure models as much variance as possible in the tensor. The remaining data that cannot be modeled with the single trilinear structure end up in the residual *E* matrix (Fig. 3(B)). The resulting A-component of the trilinear structure is the spatial distribution we are interested in. The B-component is the extracted time series. The C-component contains the distribution over the spikes in the tensor. Note that the meaning of the C-component for the SP-CP method is different than it was for the O-CP method, in which the third dimension was built up of wavelet coefficients instead of different EEG segments.

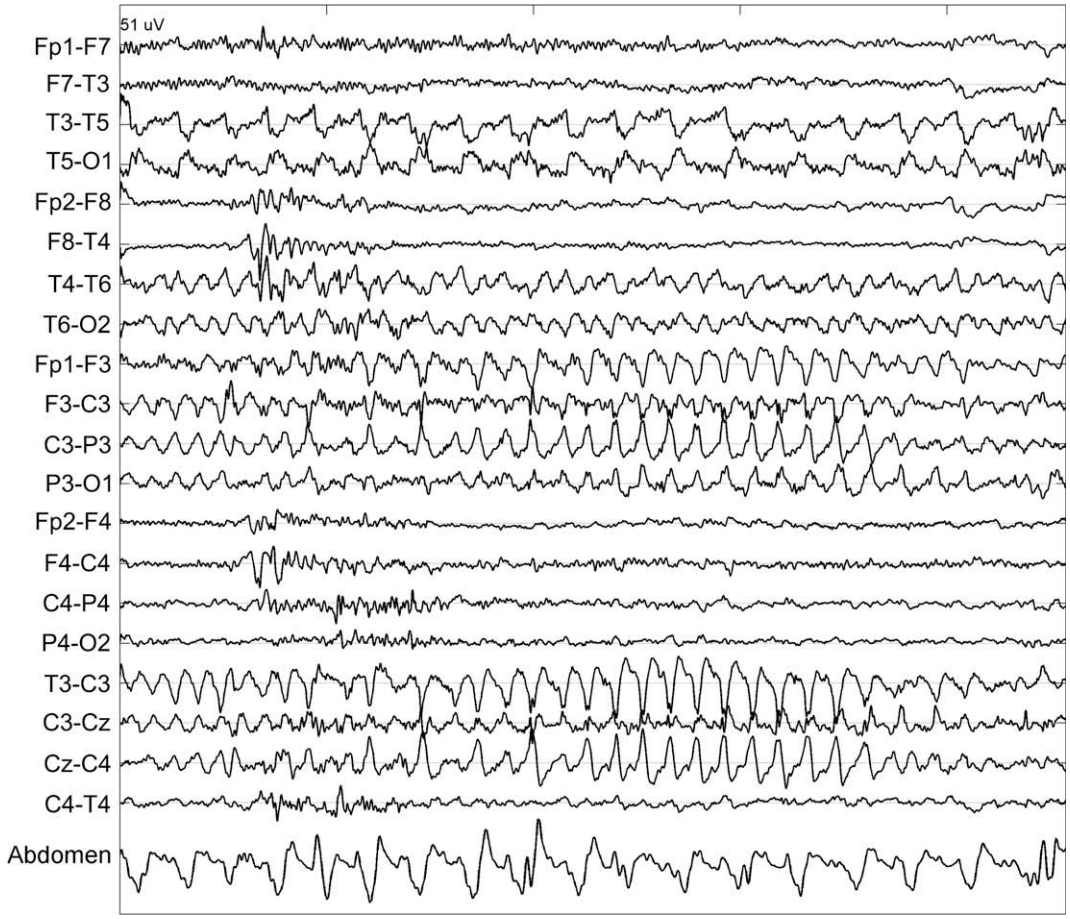


Fig. 4. Example of an oscillatory seizure predominantly present on channels T3-C3, Cz-C4, Fp1-F3, and C3-P3. Besides the seizure, a respiratory artefact is present on channels T3-T5 and T5-O1. The artefact was identified by the high correlation with the signal recorded by a sensor on the abdomen.

2.2.4. Spike triggered averaging

Another well-known method used to localize spikes is EEG 'spike triggered averaging'. This method is widely used to improve the SNR and better localize paroxysmal sharp activity, such as interictal spikes in patients with epilepsy (Bast et al., 2006) or rolandic sharp waves in neonates (Braga et al., 2002). The spatial distribution of the spikes is obtained by taking the value of the amplitude of each channel at the largest peak of the averaged spike EEG. In the results section we compare the SP-CP method with spike triggered averaging and quantify the robustness of both methods to noise.

3. Results

3.1. Illustration of the application of the O-CP method

We illustrate extraction of oscillatory sources with the O-CP method by applying this method to the EEG presented in Fig. 4. This EEG shows two dominant types of activity. Most important is the oscillatory seizure activity on channels T3-C3, Cz-C4, Fp1-F3, and C3-P3. The second strong source is a respiratory artefact on channels T3-T5 and T5-O1, which was verified by its strong correlation with the signal from a sensor on the abdomen.

The seizure activity needs to be completely separated from the artefact to obtain a reliable localization. Therefore, a two-component O-CP decomposition is calculated, implying that background EEG activity is assumed to end up in the residual variability tensor E (Eq. (1)). Fig. 5(A) shows the two extracted B-components of the CP decomposition, which correspond to the time series extracted from the EEG (Fig. 4). The signal at the top corresponds to the extracted seizure activity, the signal at the bottom to the slower respiratory artefact. Fig. 5(B) shows the topographic representation of the extracted spatial distributions or A-components in the CP decomposition. Fig. 5(B-1) corresponds to the location of the left-central seizure activity, while Fig. 5(B-2) corresponds to the left posterior temporal location of the respiratory artefact. Separation between the two oscillatory sources is possible as they have different spatial and frequency properties, implying that they cannot be accurately modeled with a single trilinear structure. In order to model the variance in the tensor properly, the CP decomposition must "accommodate" the different oscillations within different trilinear structures.

3.2. Illustration of the application of the SP-CP method

The application of the SP-CP method is illustrated by applying it to the EEG and detected spikes displayed in Fig. 6. Visual analysis indicates that the spikes originate from the left anterior temporal brain region. The result of the SP-CP algorithm is shown in Fig. 7.

Fig. 7(A) is the A-component of the CP decomposition (see Fig. 3(B)). The A-component corresponds to the spatial distribution and can be plotted as a topographic plot. The location of the extracted activity is left anterior temporal, which corresponds to the location obtained by visual analysis of the EEG in Fig. 6. Fig. 7(B) illustrates the B-component of the CP decomposition. This component is the extracted time series and can be viewed as a prototype for the detected spikes. Fig. 7(C) is the C-component of the CP decomposition. This curve represents the distribution of the extracted time series over all spikes (73 spikes were detected) in the tensor. The arrows indicate the few spikes that have a lower contribution to the extracted time series.

3.3. Robustness of the SP-CP method and comparison with spike triggered averaging

The following simulations illustrate the robustness of the SP-CP method in comparison with spike triggered averaging. In the first simulation, we constructed a tensor consisting of 5 identical EEG spike segments. We then replaced the third slice in the tensor by uniform random noise and calculated the CP decomposition of this tensor. The C-component of the decomposition is plotted in Fig. 8(A). This C-component corresponds to the weight of each EEG spike

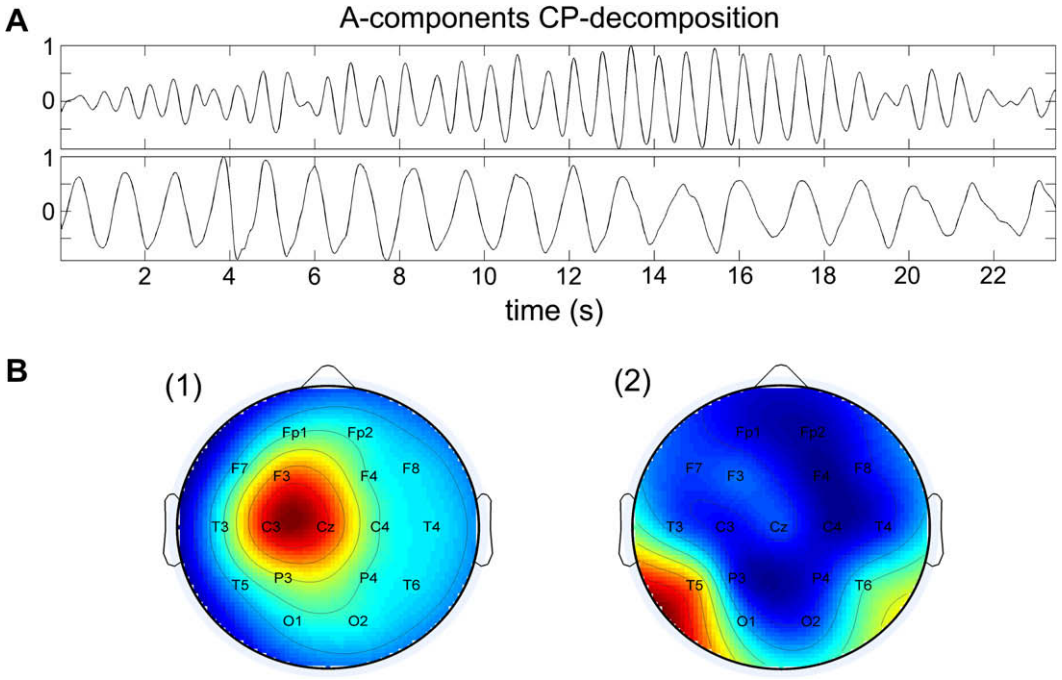


Fig. 5. Result of the O-CP algorithm on the EEG in Fig. 4. (A) The upper curve is the extracted time course corresponding to the seizure activity and the lower to the respiratory artefact. (B) Topographic plots of the extracted spatial distribution corresponding to (B-1) the seizure activity and (B-2) the artefact activity. Note that the artefact does not contaminate the seizure localization as there is no temporal activity on B-1.

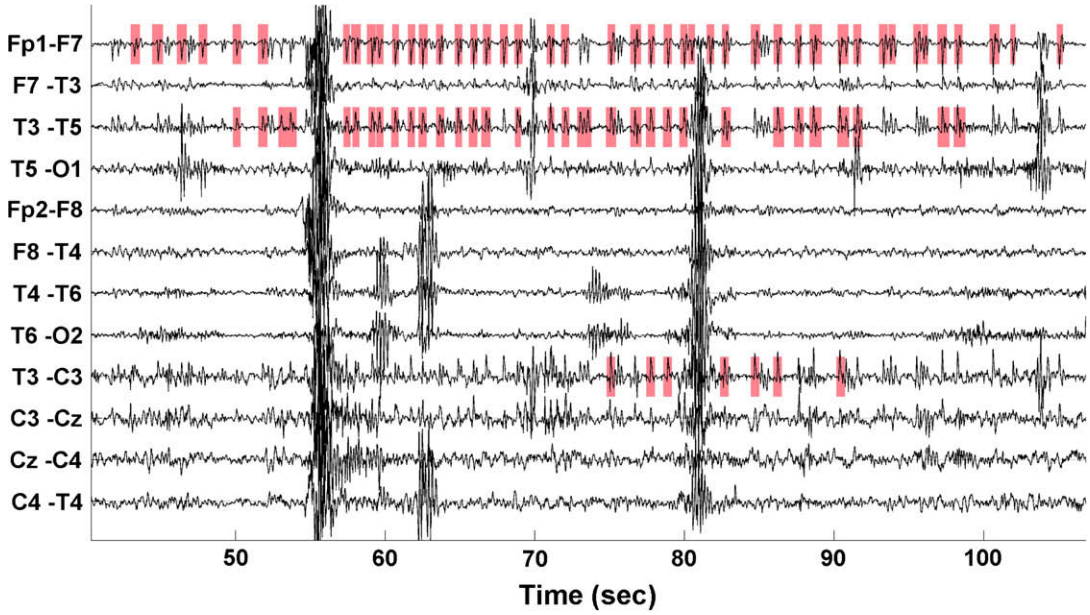


Fig. 6. Example of a spike train type seizure and result of the automated detection algorithm. The segments detected by the spike train detection algorithm are marked in red. The seizure is located on channels Fp1-F7, T3-T5, and T3-C3.

segment to the localization, similar as the C-component plotted in Fig 7(C). Fig. 8(A) demonstrates that slices 1, 2, 4, and 5 contribute equally (because they are identical), but slice 3 (the one with uniform noise) has a contribution that is 50 times lower than that of the other slices. This simulation illustrates that when an EEG slice does not correspond to the global variance in the tensor, it is assigned a very low weight and, hence, a low contribution to the extracted localization. In spike triggered averaging, this is not the case as each spike segment carries an equal weight to the averaged result.

This advantage over spike triggered averaging can be further illustrated by analyzing how both methods behave when noise is added to all slices of the tensor. We measured the influence of the noise by calculating the correlation between the extracted spatial localization (A-component) when no noise is added and the one with added noise. When the noise has no influence on the localization, this correlation is equal to 1. The result is shown in Fig. 8(B). At high SNR, the spike triggered averaging has comparable performance to the SP-CP method, with the correlation being very close to or equal to 1. However, at an SNR of 0 dB, i.e., when the power of the noise equals that in the spike, the performance of the spike triggered averaging method starts to drop significantly, while the correlation of the SP-CP method remains close to 1.

3.4. Comparison with visual analysis of the EEG

Fig. 9 shows the topographic plots of 2 seizures for each patient together with a textual indication of the relevant electrode positions defined by visual analysis of the plot. Table 1 shows the results of the visual analysis of the EEG by the clinical neurophysiologist and the visual analysis of the topographic plots (of which Fig. 9 shows 2 examples for each patient). Whether the O-CP or SP-CP method is used to localize the seizure is entirely based on the detection by the seizure detector (Deburchgraeve et al., 2008). The EEG trace marked by this detector as seizure EEG is used as input to the respective method without any manual selection. A few seizures were detected by both algorithms. In

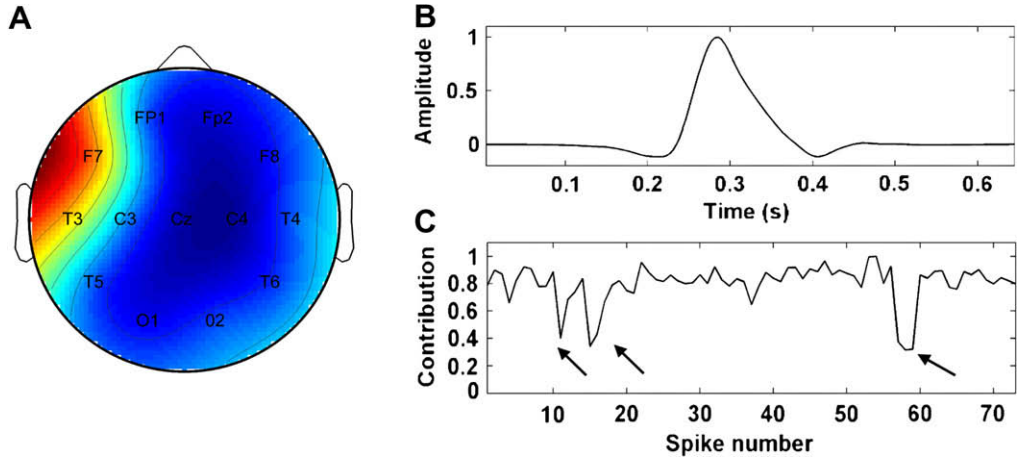


Fig. 7. (A) A-component of the CP decomposition (see Fig. 3(B). The A-component corresponds to the spatial distribution of the spikes and can be plotted as a topographic plot. The location of the extracted activity is left anterior temporal. (B) SP-CP extracted time series (B-component) with similar morphology to the detected spikes. (C) C-component of the CP decomposition. This curve represents the distribution of the extracted time series over all spikes (73 spikes were detected) in the tensor. The arrows indicate the few spikes that have a lower contribution to the extracted time series.

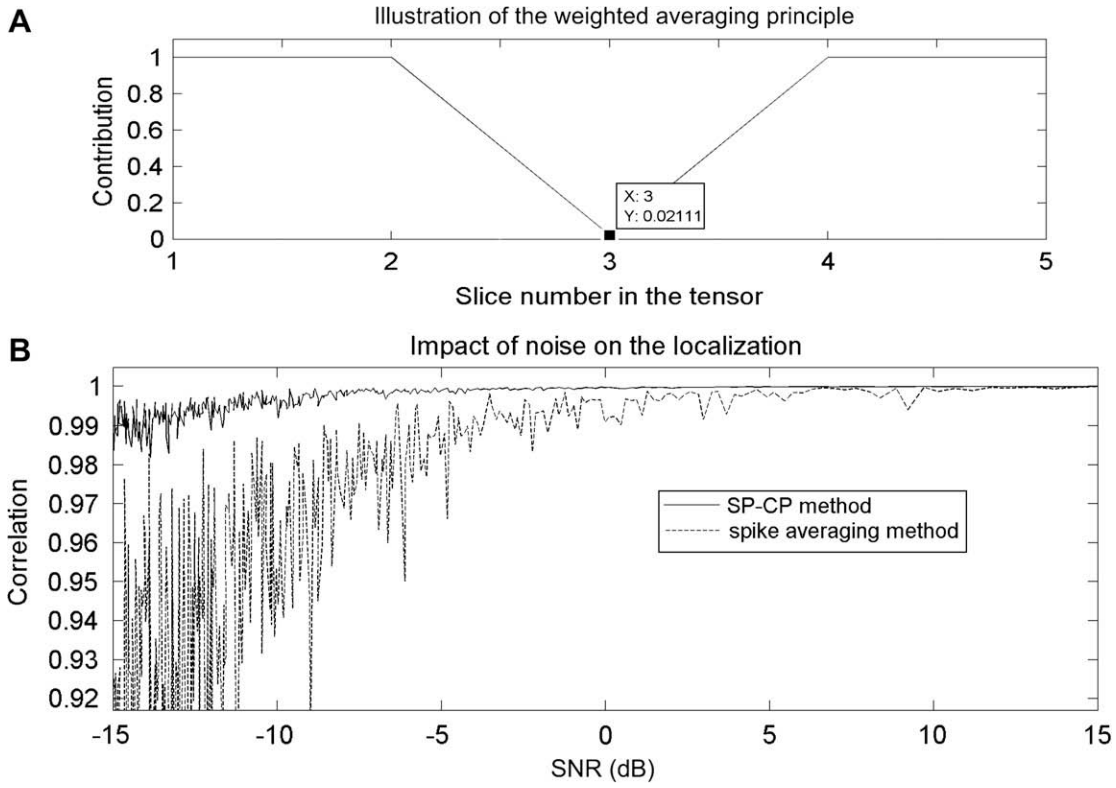


Fig. 8. Illustration of the robustness of the SP-CP method. (A) C-component of the CP decomposition of a tensor consisting of 4 identical slices (slices 1, 2, 4, and 5) and random noise on the 3rd. The weight of the 3rd slice is very low compared to that of the other slices, indicating that the CP method does not use this slice to model the variance in the tensor. In spike averaging, each slice gets an equal weight. This difference makes the SP-CP method less sensitive to noise. (B) Illustration of the robustness of the SP-CP method to noise added to the tensor. Even at high SNR, the extracted SP-CP localization remains close to the localization without noise (correlation equal to 1). At low SNR, the spike averaging method is much more influenced by the noise than the SP-CP method.

those cases, both localization methods were used and compared to the visual analysis.

4. Discussion

In this paper, we introduce two methods to localize neonatal seizures. Each method was designed to handle a specific seizure type. Both use the CP decomposition methodology to extract information regarding the localization of the source of the seizure as reflected on the scalp. The O-CP method was designed to extract and localize the oscillatory type of seizures; the SP-CP was designed to localize spike train activity. The two methods use a 3-dimensional tensor in which the first two dimensions are space and time, but differ in the construction of the third dimension. The O-CP method decomposes the EEG into different frequency components, and the SP-CP method constructs the third dimension by arranging all detected EEG spike segments one after the other. Thus, each method uses the specific features of the seizure type it is designed to localize. We also show that these methods can differentiate seizure activity from artefact and the SP-CP method, when compared to simple spike averaging, is resistant to the effect of random noise.

4.1. Application of both methods to the same seizure

We used a different localization method for oscillatory or spike train type seizure, based on their morphological characteristics. However, some neonatal seizures consist of a combination of the two seizure types. Those seizures can be localized using either method. In the results shown in Table 1, we have included a number of seizures which were localized with both methods (patient 4, seizure 1, 2; and patient 6, seizure 1, 2). We can conclude that both methods give, as expected, similar results.

4.2. Dynamic seizures

The methods assume a fixed localization for the complete window of analysis. This is a potential limitation in case of dynamic seizures that spread or migrate from one brain region to another. Epileptic seizures in adults and older children frequently behave in this way. However, neonatal seizures tend to have a comparatively limited electrographic spread (Bye and Flanagan, 1995; Patrizi et al., 2003). This is probably because the connectivity between different brain regions is not well-developed in the immature brain (Kostovic and Jovanov-Milosevic, 2006). In those cases where there is some spreading of the seizure, it is necessary to divide the seizure in possibly overlapping windows. The CP decomposition methods should then be applied to each window to localize the seizure more accurately, and to track it in time. Algorithms that enable such tracking have recently described (Nion and Sidiropoulos, 2009). In case a CP decomposition is made on a seizure that starts in one brain region and ends in another, De Vos et al. (2007b) proved with simulations that the CP decomposition will model the seizure location somewhere in the middle, as one can intuitively expect. Secondly, the active region of the seizure may become larger in time, meaning that the seizure spreads to more neighboring electrodes. This spreading is not a real problem for localization, as the major location of the seizure stays the same; it is only the spread of the seizure to other electrodes that becomes stronger over time.

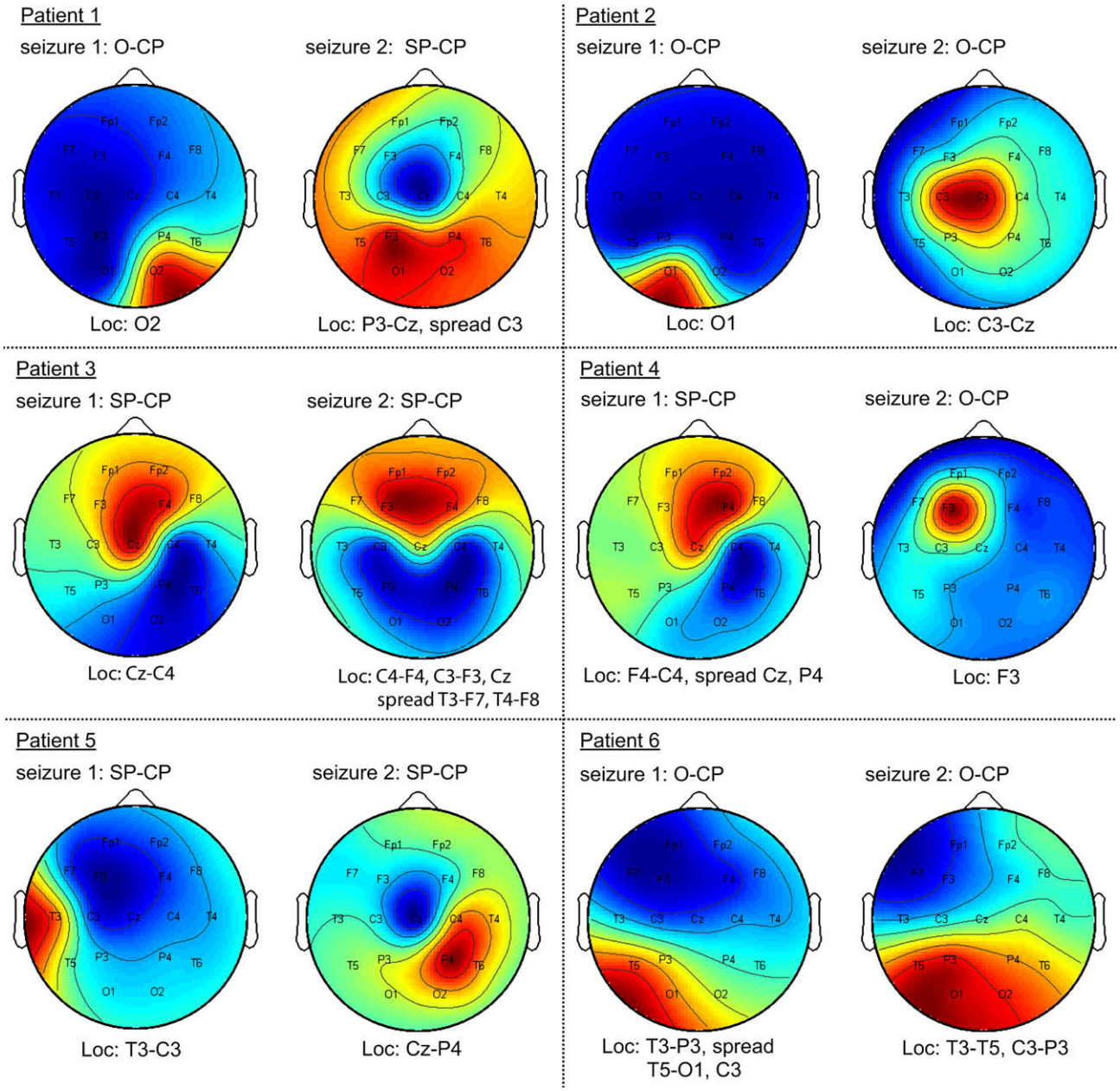


Fig. 9. Locations (Loc) of the seizures determined by the topographic plots of the SP-CP and O-CP algorithms (see also Table 1). The algorithm used to localize the seizure is mentioned above each topographic plot.

4.3. Interpretation of the topographic plots

If there is a strong difference in polarity visible on the topographic plots (clear difference between positive (red) and negative (blue) brain regions) then the isopotential lines in between those regions indicate the location of the seizure on the scalp (e.g. Fig. 9, patient 5, seizure 2 with localization between Cz-P4). Seizures localized to the edge of the topographic map (e.g. Fig. 9, patient 1, seizure 1 with localization on O2) have only 1 strongly localized polarity, the opposite polarity is more diffusely distributed as it is directed away from the electrodes. This region of the brain is not encompassed by a complete array of surrounding electrodes thus a sharp cutoff between the two polarities as seen in seizure 1 cannot be obtained. Another situation is when there is a strong polarity expressed close to the midline (e.g. patient 2, seizure 2) without clear difference between opposing polarities. This is because the opposite polarity is directed towards deeper brain regions and thus not visible on a 2D plot. These limitations are introduced due to the way scalp EEG is recorded and not due to limitations of the algorithm.

4.4. Comparison between topographic plots and visual analysis of the EEG

Table 1 shows the comparison between the visual analysis of seizures by the clinical neurophysiologist and the topographic plots of the algorithms. This similarity is difficult to quantify, but qualitatively, there is a good agreement between the two methods. For instance, seizure 1 of patient 3 shown on Fig. 9 clearly originates from the right side of the brain between channels Cz-C4, while seizure 2 affects both hemispheres. This can especially be of help to non-expert readers of the EEG, such as NICU personnel,

Table 1
Results of the comparison between visual analysis of the EEG by the clinical neurophysiologist and visual analysis of the topographic plots produced by the algorithms.

Patient	Seizure	Analysis	Location Algorithm	Location Clinical neurolophysiologist
1	1	O-CP	O2	O2
	2	SP-CP	P3-Cz, spread C3	P3, spread Cz-C3
	3	SP-CP	P3-Cz	Cz-P3
	4	SP-CP	P3-Cz	Cz
	5	SP-CP	P3-Cz, spread C3	Cz-C3, spread P3
2	1	O-CP	O1	O1
	2	O-CP	C3-Cz	C3-Cz
	3	O-CP	O2	O2
	4	O-CP	O1	O1
	5	O-CP	Cz, spread P3-P4	Cz, spread C3-C4
3	1	SP-CP	Cz-C4	Cz-C4
	2	SP-CP	C4-F4, C3-F3, Cz spread T3-F7, T4-F8	C4, spread F8,T3
	3	SP-CP	C3-F3, Cz-C4	Cz-C4, spread F3
4	1	SP-CP	F4-C4, spread Cz,P4	Cz-C4
		O-CP	Cz-C4, spread F4, P4	Cz-C4
	2	O-CP	F3	F3-C3
		SP-CP	F3	F3-C3
5	1	SP-CP	T3-C3	T3
	2	SP-CP	Cz-P4	Cz
	3	SP-CP	Cz-C4	Cz-C4
6	1	O-CP	T3-P3, spread T5-O1, C3	T5-O1
		SP-CP	T3-P3, spread T5-O1, C3	T5-O1
	2	O-CP	T3-T5, C3-P3	T5-O1, spread P3
		SP-CP	T3-T5, C3-P3	T5-O1, spread P3
	3	SP-CP	F4-F8, C4-T4	F8-T4

who can derive such information much more readily from the topographic plots than by looking at the raw EEG.

4.5. Practical applications of the methods

The algorithms presented in this paper can be used in the NICU together with the previously developed seizure detector to form a complete seizure monitoring system. Such monitoring can yield important prognostic information. E.g. seizure burden, length of seizure discharges (Connell et al., 1989), number of seizure foci present (Bye et al., 1997), spread of seizures to contralateral hemisphere (Pisani et al., 2008), etc. Visually scoring the EEG to obtain this information for use in the NICU is labor-intensive and happens seldom in clinical practice. Automated monitoring as presented here can therefore be a valuable addition to current monitoring practice.

We are presently studying if there is a relationship between the location of the neonatal seizures and the location of the structural brain damage as seen on imaging techniques such as MRI and ultrasonogram (Biagioni et al., 2001). For such research purposes, the algorithms can be combined with dipole source localization (Merlet and Gotman, 1999; Gotman, 2003; Michel et al., 2004) in a realistic head model (Despotovic et al., in press). There is controversy whether (neonatal) seizures can be modeled with a dipole and realistic conductivity values for the neonatal brain are not yet at hand. Even with these limitations, we feel that source localization is a useful tool in exploring the link between the location of structural brain damage and neonatal seizures. It will also help in prognostication in the NICU setting and may help guide treatment in the future.

Acknowledgements

Research supported by:

- A PhD grant of the Institute for the Promotion of Innovation through Science and Technology in Flanders (IWT-Vlaanderen).
- Research Council KUL:GOA-AMBioRICS, CoE EF/05/006 Optimization in Engineering (OPTEC), IDO 05/010 EEG-fMRI, IOF-KP06/11 FunCopt, several PhD/postdoc & fellow grants;
- Flemish Government: FWO: PhD/postdoc grants, projects, G.0407.02 (support vector machines), G.0360.05 (EEG, Epileptic), G.0519.06 (Noninvasive brain oxygenation), FWO-G.03 21.06 (Tensors/Spectral Analysis), G.0302.07 (SVM), G.0341.07 (Data fusion), research communities (ICCoS, ANMMM); IWT: TBM070713-Accelero, TBM-IOTA3, PhD Grants;
- Belgian Federal Science Policy Office IUAP P6/04 (DYSCO, 'Dynamical systems, control and optimization', 2007–2011);
- EU: BIOPATTERN (FP6-2002-IST 508803), ETUMOUR (FP6-20 02-LIFESCIHEALTH 503094), Healthagents (IST-2004-27214), FAST (FP6-MC-RTN-035801), Neuromath (COST-BM0601)
- ESA: Cardiovascular Control (Prodex-8 C90242)

References

Acar E, Aykut-Bingol C, Bingol H, Bro R, Yener B. Multiway analysis of epilepsy tensors. Bioinformatics 2007;23:10–8.

Bast T, Boppel T, Rupp A, Harting I, Hoechstetter K, Fauser S, et al. Noninvasive source localization of interictal EEG spikes: effects of signal-to-noise ratio and averaging. Clin Neurophysiol 2006;23:487–97.

Biagioni E, Mercuri E, Rutherford M, Cowan F, Azzopardi D, Frizone M, et al. Combined use of electroencephalogram and magnetic resonance imaging in full-term neonates with acute encephalopathy. Pediatrics 2001;107:461–8.

Braga NIO, Manzano GM, Nobrega JAM. A comparison between averaged spikes and individual visually-analyzed spikes in rolandic epileptiform discharges. Arq Neuropsiquiatr 2002;60:699–701.

Bye AM, Flanagan D. Spatial and temporal characteristics of neonatal seizures. Epilepsia 1995;36:1009–16.

Bye AM, Cunningham CA, Chee KY, Flanagan D. Outcome of neonates with electrographically identified seizures, or at risk of seizures. Pediatr Neurol 1997;16(3):225–31.

Connell J, Oozeer R, de Vries L, Dubowitz LM, Dubowitz V. Continuous EEG monitoring of neonatal seizures: diagnostic and prognostic considerations. Arch Dis Child 1989;64(4):452–8.

Deburchgraeve W, Cherian PJ, De Vos M, Swarte RM, Blok JH, Visser GH, et al. Automated neonatal seizure detection mimicking a human observer reading EEG. Clin Neurophysiol 2008;119:2447–54.

De Clercq W, Vergult A, Vanrumste B, Van Paesschen W, Van Huffel S. Canonical correlation analysis applied to remove muscle artifacts from the electroencephalogram. IEEE Trans Biomed Eng 2006;53:2583–7.

Despotovic I, Hallez H, Vansteenkiste E, Deburchgraeve W, Philips W. Development of a realistic head model for EEG event-detection and source localization in newborn infants. In: IEEE Engineering in Medicine and Biology Society (EMBC); 2009 [in press].

De Vos M, Vergult A, De Lathauwer L, De Clercq W, Van Huffel S, Dupont P, et al. Canonical decomposition of ictal scalp EEG reliably detects the seizure onset zone. NeuroImage 2007a;37:844–54.

De Vos M, De Lathauwer L, Vanrumste B, Van Huffel S, Van Paesschen W. Canonical decomposition of ictal scalp EEG and accurate source localisation: principles and simulation study. Comput Intell Neurosci 2007:58253.

Gotman J. Noninvasive methods for evaluating the localization and propagation of epileptic activity. Epilepsia 2003;44:21–9.

Hellstrom-Westas L, Rosen I, Swenningsen NW. Silent seizures in sick infants in early life. Diagnosis by continuous cerebral function monitoring. Acta Paediatr Scand 1985;74:741–8.

Kostovic I, Jovanov-Milosevic N. The development of cerebral connections during the first 20–45 weeks' gestation. Semin Fetal Neonatal Med 2006;11:415–22.

Kovacevic N, McIntosh AR. Groupwise independent component decomposition of EEG data and partial least square analysis. NeuroImage 2007;35:1103–12.

Lanska MJ, Lanska DJ. Neonatal seizures in the United States: results of the National Hospital Discharge Survey, 1980–1991. Neuroepidemiology 1996;15:117–25.

Merlet I, Gotman J. Reliability of dipole models of epileptic spikes. Clin Neurophysiol 1999;110:1013–28.

Michel C, Murray M, Lantz G, Gonzales S, Spinelli L, Grave de Peralta R. EEG source imaging. Clin Neurophysiol 2004;115:2195–222.

Miwakeichi F, Martinez-Montes E, Valdés-Sosa PA, Nishiyama N, Mizuhara H, Yamaguchi Y. Decomposing EEG data into space–time–frequency components using parallel factor analysis. Neuroimage 2004;22:1035–45.

Murray DM, Boylan GB, Ali I, Ryan CA, Murphy BP, Connolly S. Defining the gap between electrographic seizure burden, clinical expression and staff recognition of neonatal seizures. Arch Dis Child Fetal Neonatal 2008;93:187–91.

Nion D, Sidiropoulos ND. Adaptive algorithms to track the PARAFAC decomposition of a third-order tensor. IEEE Trans on Signal Processing 2009;57(6):2299–310.

Patel A, Alotaibi F, Blume WT, Mirsattari SM. Independent component analysis of subdurally recorded occipital seizures. Clin Neurophysiol 2008;119:2437–46.

Patrizi S, Holmes LG, Orzalesi M, Allemand F. Neonatal seizures: characteristics of EEG ictal activity in preterm and fullterm infants. Brain Dev 2003;25:427–37.

Pisani F, Copioli C, Di Gioia C, Turco E, Sisti L. Neonatal seizures: relation of ictal video-electroencephalography (EEG) findings with neurodevelopmental outcome. J Child Neurol 2008;23:394–8.

Pisani F, Orsini M, Braibanti S, Copioli C, Sisti L, Turco EC. Development of epilepsy in newborns with moderate hypoxic–ischemic encephalopathy and neonatal seizures. Brain Dev 2009;31:64–8.

Rennie JM, Chorley G, Boylan GB, Pressler R, Nguyen Y, Hooper R. Non-expert use of the cerebral function monitor for neonatal seizure detection. Arch Dis Child Fetal Neonatal 2004;89:37–40.

Scher MS, Painter MJ, Bergman I, Barmada MA, Brunberg J. EEG diagnoses of neonatal seizures: clinical correlations and outcome. Pediatr Neurol 1989;5:17–24.

Smilde A, Bro R, Geladi P. Multi-way analysis with applications in the chemical sciences. John Wiley & Sons; 2004.

Tomasi G, Bro R. A comparison of algorithms for fitting the PARAFAC model. Comput Stat Data Anal 2006;50:1700–34.

Volpe JJ. Neurology of the newborn. 5th ed. Philadelphia: Saunders WB; 2008.